

# UC Santa Barbara

## UC Santa Barbara Previously Published Works

### Title

Chiral Bifunctional Phosphine Ligand-Enabled Cooperative Cu Catalysis: Formation of Chiral  $\alpha,\beta$ -Butenolides via Highly Enantioselective  $\gamma$ -Protonation

### Permalink

<https://escholarship.org/uc/item/7zt2z897>

### Journal

Journal of the American Chemical Society, 143(29)

### ISSN

0002-7863

### Authors

Cheng, Xinpeng  
Li, Tianyou  
Gutman, Kaylaa  
[et al.](#)

### Publication Date

2021-07-28

### DOI

10.1021/jacs.1c05781

Peer reviewed



Published in final edited form as:

*J Am Chem Soc.* 2021 July 28; 143(29): 10876–10881. doi:10.1021/jacs.1c05781.

## Chiral Bifunctional Phosphine Ligand-Enabled Cooperative Cu Catalysis: Formation of Chiral $\alpha,\beta$ -Butenolides via Highly Enantioselective $\gamma$ -Protonation

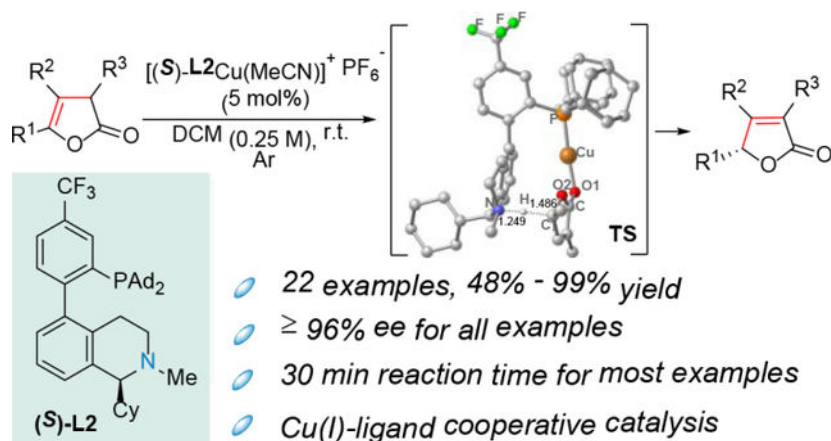
Xinpeng Cheng, Tianyou Li, Kaylaa Gutman, Liming Zhang

Department of Chemistry & Biochemistry, University of California, Santa Barbara, Santa Barbara, California 93106, United States

### Abstract

$\alpha,\beta$ -Butenolides with 96% enantiomeric excess are synthesized from  $\beta,\gamma$ -butenolides via a novel Cu(I)-ligand cooperative catalysis. The reaction is enabled by a chiral biphenyl-2-ylphosphine ligand featuring a remote tertiary amino group. DFT studies support the cooperation between the metal center and the ligand basic amino group during the initial soft deprotonation and the key asymmetric  $\gamma$ -protonation. Remarkably, other coinage metals, i.e., Ag and Au, can readily assume the same role as Cu in this asymmetric isomerization chemistry.

### Graphical Abstract



Corresponding Author zhang@chem.ucsb.edu.

Notes

The authors declare no competing financial interests.

Metrical parameters for the structures  $\{[(S)\text{-L}2\text{Cu}]_2\text{H}_2\text{O}\}^{2+} (\text{PF}_6^-)_2$  are available free of charge from the Cambridge Crystallographic Data Centre under reference numbers CCDC-2052076

ASSOCIATED CONTENT

Supporting Information

Experimental details, compound characterization, and spectra. This material is available free of charge via the Internet at <http://pubs.acs.org>.

Experimental procedures and characterization data, computational study results, Cartesian coordinates, and spectral data (PDF)  
Crystal data for  $\{[(S)\text{-L}2\text{Cu}]_2 \cdot \text{H}_2\text{O}\}^{2+} (\text{PF}_6^-)_2$  (CIF)

Many natural products featuring chiral  $\alpha$ ,  $\beta$ -butenolide motifs possess various biological activities (Scheme 1A). For example, avenolide can control the production of antibiotics in *Streptomyces avermitilis*,<sup>1</sup> thorectandrols B inhibits the growth of MALME-3M (melanoma) and MCF-7 (breast) cancer cell lines,<sup>2</sup> and kallolide A exhibits anti-inflammatory activity.<sup>3</sup> Various synthetic approaches have been developed to access chiral  $\alpha,\beta$ -butenolide.<sup>4</sup> The direct catalytic olefin isomerization of racemic/achiral  $\beta,\gamma$ -butenolide into chiral  $\alpha,\beta$ -butenolide via the achiral 2-furanoxyl anion **A** is an atom-economic and arguably the simplest approach (Scheme 1B), yet has been only sparsely explored. A notable advance in this strategy was achieved by Deng<sup>5</sup> in 2011 by employing a cinchona-derived organocatalyst. In this chemistry, good levels of enantioselectivities (87–94% ee) are achieved for  $\gamma$ -monosubstituted and  $\alpha$ ,  $\gamma$ -disubstituted  $\alpha$ ,  $\beta$ -butenolide products, but only moderate ee values (81–82%) are reported for the  $\beta,\gamma$ -disubstituted  $\alpha,\beta$ -butenolides. This chemistry was applied in the total synthesis of Leucosceptroid family of natural products,<sup>6</sup> where a moderate diastereomeric ratio of 7/1 was reported with the latter butenolide type. Herein, we report a Cu(I)-bifunctional phosphine cooperative catalysis that achieves the asymmetric butenolide isomerization which exhibits enantiomeric excess ranging from 96% to 99%. Moreover, this chemistry is applicable to all of the three aforementioned substitution patterns and proceeds at ambient temperature and mostly in 0.5 h.

For the past several years, we<sup>7</sup> have developed various bifunctional biphenyl-2-ylphosphine ligands<sup>8</sup> featuring a remote basic group for gold-ligand cooperative catalysis.<sup>8–9</sup> Scheme 1C shows the chiral ligands that have enabled asymmetric cooperative gold catalysis.<sup>8a,8c,8e</sup> Among them, **L2** and **L3** feature a fluxional biphenyl axis and a remote tertiary amino group possessing an  $\alpha$ -chiral center and engaging in critical propargylic deprotonation during catalysis, as revealed by the DFT-optimized TS **B** using (*S*)-**L3** as the ligand.<sup>8e</sup> Despite the syn-periplanar nature of the concerted Au-activation and amino-deprotonation, we envisioned that an orthogonal organization of a ‘pulling’ cationic metal and a ‘pushing’ basic amino group can be readily achieved by these chiral ligands, as outlined in the structures **C** and **C'** in Scheme 1D, which should be suited for soft enolization and the reverse protonation. This protonation of the metal enolate could be extended to the  $\gamma$ -protonation of the metal 2-furanolate in **D**. As such, we envision that chiral ligands such as **L2** or **L3** might enable highly enantioselective isomerization of  $\beta,\gamma$ -butenolides via sequential soft enolization and asymmetric  $\gamma$ -protonation.<sup>10</sup> Since Cu<sup>I</sup> and Ag<sup>I</sup> can also adopt the same linear bis-coordinated structures with bulky phosphine,<sup>11</sup> we anticipate that the corresponding Cu<sup>I</sup> or Ag<sup>I</sup> complexes featuring these bifunctional ligands could also be effective in this cooperative catalysis manifold.<sup>12</sup> Moreover, these harder and cheaper coinage metals may be advantageous in enolate chemistry over softer Au since the coordination/activation of hard carbonyl oxygen instead of soft C-C triple bond is desired. It is noteworthy that metal-ligand cooperative catalysis involving Cu<sup>I</sup><sup>13</sup> or Ag<sup>I</sup> is scarce, and this design, if implemented, would constitute the first application of this class of bifunctional ligands in Cu or Ag catalysis.

Guided by these considerations, we initiated our investigation by employing Cu as the metal and the  $\beta$ ,  $\gamma$ -butenolide **1a** – prepared from an allenic ester in two steps<sup>5</sup> – as the model substrate. As expected, the Cu<sup>I</sup> salt, [Cu(MeCN)<sub>4</sub>]<sup>+</sup> PF<sub>6</sub><sup>–</sup>, alone could not promote

the isomerization of **1a** into the  $\alpha,\beta$ -butenolide product **2a** to a noticeable extent (entry 1), nor was its combination with Et<sub>3</sub>N (entry 2). [JohnPhosCu(MeCN)]<sup>+</sup> PF<sub>6</sub><sup>-11b</sup> and Et<sub>3</sub>N (5 mol % each) did lead to substantial conversion in 16 h at ambient temperature, albeit in 6% yield (entry 3). The reaction was, however, drastically improved when JohnPhos was replaced by the achiral tertiary amine-functionalized ligand **L4**.<sup>8b</sup> With the *in-situ* generated **L4**Cu<sup>+</sup>, the reaction proceeded to completion in 3 h and afforded **2a** in nearly quantitative yield (entry 4). This large enhancement of reactivity is consistent with the intended Cu-ligand cooperation. When the chiral ligand (*S*)-**L2** along with [Cu(MeCN)<sub>4</sub>]<sup>+</sup> PF<sub>6</sub><sup>-</sup> was employed, the reaction again proceeded with excellent efficiency and moreover, the *ee* of **2a** was 98% (entry 5). The (*R*)-configuration of **2a** is inferred by comparing the specific optical rotations of its homologs **2b** and **2c** (see Table 2) with the literature data.<sup>5</sup> The replacement of (*S*)-**L2** with (*S*)-**L3**<sup>8e</sup> led to 94% *ee* (entry 6). To establish the structure of the Cu(I) catalyst, we prepared [(*S*)-**L2**Cu(MeCN)]<sup>+</sup> PF<sub>6</sub><sup>-</sup> by following the related protocol for [JohnPhosCu(MeCN)]<sup>+</sup> PF<sub>6</sub><sup>-</sup>.<sup>11b</sup> With this preformed chiral cationic Cu(I) complex as the catalyst, the reaction time was shortened to 1 h, while the yield and *ee* remained excellent (entry 7). Performing the reaction under argon atmosphere further shortened the reaction time to 30 min (entry 8). This observation is consistent with Cu(I) catalysis as atmospheric oxygen might oxidize Cu(I) to likely nonreactive Cu(II). To further characterize the Cu(I) catalyst, we obtained its single crystals for X-ray diffraction studies. However, the solved structure, as shown in Figure 1, is a dimeric (*S*)-**L2**Cu(I) complex with the two-metal center bridged by a molecule of water. Nevertheless, it confirms that the Cu(I) center is bis-coordinated, with the angles of P-Cu-O being 167.8° and 163.2°, respectively. This structural feature supports our reaction design. Moreover, this dimeric complex is equally effective as the catalyst (entry 9). In the control experiments, the ligand itself was not competent (entry 10), and Cu(II) salts such as Cu(OTf)<sub>2</sub> and Cu(hfac)<sub>2</sub> could not serve as the copper source (entry 11). Interestingly, this catalytic system worked equally well with the other coinage metals. Hence, with Ag<sup>I</sup> or Au<sup>I</sup> at the metal center, nearly identical results were obtained (entries 12 and 13). This interchangeability among the coinage metals is remarkable and rare. The scalability of this Cu(I) catalysis was demonstrated on a gram-scale reaction in entry 14. With 1 mol % of the catalyst, the reaction was completed in one hour and delivered 0.99 g of **2a** in 92% yield and with 99% *ee*.

With the optimized reaction conditions (i.e., Table 1, entry 8) in hand, we set out to explore the reaction scope. As shown in Table 2, a series of  $\alpha,\gamma$ -disubstituted  $\alpha,\beta$ -butenolides (**2b-2o**) were synthesized in yields ranging from 88% to 99% and with 96% *ee*. The R<sup>1</sup> group in this series can accommodate methyl (**2b**), isopropyl (**2c**), bulky t-butyl group (**2d**), and various functional groups including C-C double bonds (**2e** and **2f**), phenyl (**2g**), thiophen-2-yl (**2h**), chloro (**2i**), phenyloxy (**2j**), and phenylthio (**2k**). From the substrate prepared from (*S*)- $\beta$ -citronellol, (*5S, 2'S*)-**2l** was formed with 99% diastereomeric excess when (*S*)-**L2** was employed. By switching the chiral ligand to its enantiomer, the diastereomer (*5R, 2'S*)-**2l** was formed with the same level of excellent diastereoselectivity. This ligand-enabled diastereomeric divergence permits flexible and selective access to stereochemical arrays. Little impact on the reactivities was noticed when the R<sup>3</sup> group was switched from methyl (**2a**) to allyl (**2m**), prenyl (**2n**), or benzyl groups (**2o**).

Next, we turned our attention to the synthesis of  $\beta$ ,  $\gamma$ -disubstituted  $\alpha$ ,  $\beta$ -butenolides (**2p-2s**). Much to our delight, they were also formed with 97% ee. The  $\beta$ -substituent, i.e.,  $R^2$ , can be sterically demanding isopropyl (**2q**) or part of 6-/7-membered ring connected to the  $\gamma$  substituent (**2r** and **2s**).

Finally, the preparation of chiral monosubstituted  $\alpha$ ,  $\beta$ -butenolides (**2t** and **2u**) was examined. As expected, in the absence of  $\alpha$ - and/or  $\beta$ -substituents to stabilize the product double bond, the energy differences between the substrates and the products appear to be small. As such, this asymmetric isomerization was sluggish and could not reach full conversion due to reaction equilibrium. 40 °C and 17 h were employed to improve the reaction yields without compromising the exceptional enantioselectivity. Due to volatility, the isolated yield of **2u** was moderate.

In comparison to literature results,<sup>5</sup> which are shown in red in Table 2, this asymmetric Cu(I) catalysis displays marked improvement in asymmetric induction. The difference is particularly significant in the cases of the  $\beta$ , $\gamma$ -disubstituted  $\alpha$ , $\beta$ -butenolides **2p** and **2r**, where the ee values were improved from 81% to 99% and from 82% to 97%, respectively. Moreover, the reaction conditions were substantially improved, i.e., rt and 0.5 h over -20 °C and 24 h.

The ambient NMR spectra of [(*S*)-**L2Cu**(MeCN)]<sup>+</sup> SbF<sub>6</sub><sup>-</sup> in CD<sub>2</sub>Cl<sub>2</sub> revealed a ~ 1:1 mixture of atropisomers, which is caused by the retarded rotation of its biphenyl axis. In the atropisomer with the axis configuration identical to those in the X-ray structure in Figure 1, the ligand nitrogen lone pair electrons point away from the metal center or are shielded by the  $\alpha$ -cyclohexyl group. As such, it is not catalytically active. We determined by NMR that the coalescence of the atropisomeric chemical shifts of this Cu(I) complex occurred between 60 °C and 65 °C and the rotational barrier was calculated to be 17.8 – 18.1 kcal/mol. At ambient temperature, the biphenyl axis is sufficiently fluxional and most of the catalyst should participate in the catalysis by adopting the desired axis configuration. We also examined the correlation between the ee of **2a** and the ee of [(**L2Cu**(MeCN)]<sup>+</sup> PF<sub>6</sub><sup>-</sup>. A moderate negative non-linear effect was revealed (see SI).<sup>14</sup> This phenomenon can be interpreted as the monomeric Cu(I) complex being the active catalyst and equilibrating homochiral dimeric/polymeric Cu(I) species such as {[(*S*)-**L2Cu**]<sub>2</sub>·H<sub>2</sub>O}<sup>2+</sup> (PF<sub>6</sub><sup>-</sup>)<sub>2</sub> being catalytically incompetent.<sup>15</sup>

To offer insight into the reaction mechanism and understand the extraordinary asymmetric induction, we conducted DFT studies of the reaction forming **2b** at the PBE1PBE level using the effective core potential SDD for Cu and the basis set 6-311g(d,p) for P and 6-31g(d,p) for the other atoms. The SMD model is employed for solvent DCM. As shown in Scheme 2, the deprotonation step eliminates the  $\alpha$ -chiral center of the  $\beta$ , $\gamma$ -butenolide **1b** and exhibits only a minor difference in reaction barriers. The dihedral angles of Cu-O1-C $\alpha$ -H in the transition states for the (*S*)- and (*R*)-**1b** substrates, a measure of the relative orientation of the ‘push’ and ‘pull’ in this soft enolization, are 46.9° and 72.5°, respectively, revealing deviation from orthogonality but supporting the cooperative nature of the metal and the ligand amino group in the deprotonation process. The formed (furan-2-yloxy)copper(I) intermediates **3-L2Cu** and **3'-L2Cu** are conformers and differ little in free energy. The

subsequent  $\gamma$ -protonation generates the butenolide  $\gamma$ -chiral center and the two TS differ in free energy by 7.7 kcal/mol, which is consistent with the observed excellent *ee* (i.e., 97%). In the favored TS structure **TS-(R)-2b-L2Cu** leading to the observed (*R*)-**2b**, the dihedral angle of Cu-O1-C $\gamma$ -H is 67.6°, while that for the disfavored TS is 1.1°. This stark difference in the relative orientation of Cu-O1 and C $\gamma$ -H reveals the former achieving substantially better metal-ligand cooperation and is attributed to the difference in reaction energy barriers. Additionally, the energy barrier of the preferred protonation is lower than that of deprotonating either of the **1b** enantiomers by 2.3 kcal/mol, suggesting that the stereo-eliminating deprotonation is the rate-limiting step, which is opposite to that revealed by the DFT studies of the Deng's chemistry.<sup>16</sup>

In summary, we have developed a rare Cu(I)-ligand cooperative catalysis that is enabled by a chiral bifunctional biphenyl-2-ylphosphine ligand. The reaction converts three-types of  $\beta$ ,  $\gamma$ -butenolides into chiral  $\alpha$ ,  $\beta$ -butenolides with 96% *ee*. DFT calculations support the cooperative nature between the Cu(I) center and the ligand remote amino group both in the soft deprotonation and the asymmetric  $\gamma$ -protonation steps. Remarkably, other coinage metals, i.e., Ag and Au, can be equally effective in this catalysis. We anticipate that this coinage metal-ligand cooperation approach would find broader applications in asymmetric protonation and enolate chemistry.

## Supplementary Material

Refer to Web version on PubMed Central for supplementary material.

## ACKNOWLEDGMENT

The authors thank NIH R01GM123342 and 1R35GM139640 and NSF CHE 1800525 for financial support, NSF MRI-1920299 for the acquisition of Bruker 500 MHz and 400 MHz NMR instruments, and Drs. Ting Li and Conghui Tang for conducting some initial studies on the related gold catalysis.

### Funding Sources

NIH R01GM123342, 1R35GM139640

NSF CHE 1800525, NSF MRI-1920299, CNS-1725797, DMR 1720256.

## REFERENCES

- (1)a). Kitani S; Miyamoto KT; Takamatsu S; Herawati E; Iguchi H; Nishitomi K; Uchida M; Nagamitsu T; Omura S; Ikeda H; Nihira T 'Avenolide, a Streptomyces Hormone Controlling Antibiotic Production in Streptomyces Avermitilis' Proc. Natl. Acad. Sci 2011, 108, 16410–16415; [PubMed: 21930904] b)Uchida M; Takamatsu S; Arima S; Miyamoto KT; Kitani S; Nihira T; Ikeda H; Nagamitsu T 'Total Synthesis and Absolute Configuration of Avenolide, Extracellular Factor in Streptomyces Avermitilis' J. Antibiot 2011, 64, 781–787.
- (2). Charan RD; McKee TC; Boyd MR 'Thorectandrols a and B, New Cytotoxic Sesterterpenes from the Marine Sponge Thorectandra Species' J. Nat. Prod 2001, 64, 661–663. [PubMed: 11374971]
- (3)a). Look SA; Burch MT; Fenical W; Zheng Q; Clardy J 'Kallolide a, a New Antiinflammatory Diterpenoid, and Related Lactones from the Caribbean Octocoral Pseudopterogorgia Kallos (Bielschowsky)' J. Org. Chem 1985, 50, 5741–5746;b)Marshall JA; Liao J 'Stereoselective Total Synthesis of the Pseudopterolide Kallolide A' J. Org. Chem 1998, 63, 5962–5970. [PubMed: 11672200]

- (4)a). Carter NB; Nadany AE; Sweeney JB 'Recent Developments in the Synthesis of Furan-2(5h)-Ones' *J. Chem. Soc, Perkin Trans 1* 2002, 2324–2342;b)Mao B; Fañanás-Mastral M; Feringa BL 'Catalytic Asymmetric Synthesis of Butenolides and Butyrolactones' *Chem. Rev* 2017, 117, 10502–10566. [PubMed: 28640622]
- (5). Wu Y; Singh RP; Deng L 'Asymmetric Olefin Isomerization of Butenolides Via Proton Transfer Catalysis by an Organic Molecule' *J. Am. Chem. Soc* 2011, 133, 12458–12461. [PubMed: 21766859]
- (6). Hugelshofer CL; Magauer T 'Total Synthesis of the Leucosceptroid Family of Natural Products' *J. Am. Chem. Soc* 2015, 137, 3807–3810. [PubMed: 25768917]
- (7). Cheng X; Zhang L 'Designed Bifunctional Ligands in Cooperative Homogeneous Gold Catalysis' *CCS Chem* 2020, 2, 1989–2002.
- (8)a). Cheng X; Wang Z; Quintanilla CD; Zhang L 'Chiral Bifunctional Phosphine Ligand Enabling Gold-Catalyzed Asymmetric Isomerization of Alkyne to Allene and Asymmetric Synthesis of 2,5-Dihydrofuran' *J. Am. Chem. Soc* 2019, 141, 3787–3791; [PubMed: 30789268] b)Wang Z; Ying A; Fan Z; Hervieu C; Zhang L 'Tertiary Amino Group in Cationic Gold Catalyst: Tethered Frustrated Lewis Pairs That Enable Ligand-Controlled Regiodivergent and Stereoselective Isomerizations of Propargylic Esters' *ACS Catal.* 2017, 7, 3676–3680;c)Wang Z; Nicolini C; Hervieu C; Wong Y-F; Zannoni G; Zhang L 'Remote Cooperative Group Strategy Enables Ligands for Accelerative Asymmetric Gold Catalysis' *J. Am. Chem. Soc* 2017, 139, 16064–16067; [PubMed: 29058889] d)Wang Y; Wang Z; Li Y; Wu G; Cao Z; Zhang L 'A General Ligand Design for Gold Catalysis Allowing Ligand-Directed Anti-Nucleophilic Attack of Alkynes' *Nature Commun.* 2014, doi: 10.1038/ncomms4470;e)Li T; Cheng X; Qian P; Zhang L 'Gold-Catalysed Asymmetric Net Addition of Unactivated Propargylic C–H Bonds to Tethered Aldehydes' *Nat. Catal* 2021, 4, 164–171; [PubMed: 34755042] f)Wang Z; Wang Y; Zhang L 'Soft Propargylic Deprotonation: Designed Ligand Enables Au-Catalyzed Isomerization of Alkynes to 1,3-Dienes' *J. Am. Chem. Soc* 2014, 136, 8887–8890. [PubMed: 24911158]
- (9)a). Li T; Zhang L 'Bifunctional Biphenyl-2-Ylphosphine Ligand Enables Tandem Gold-Catalyzed Propargylation of Aldehyde and Unexpected Cycloisomerization' *J. Am. Chem. Soc* 2018, 140, 17439–17443; [PubMed: 30525525] b)Zhang J-Q; Liu Y; Wang X-W; Zhang L 'Synthesis of Chiral Bifunctional Nhc Ligands and Survey of Their Utilities in Asymmetric Gold Catalysis' *Organometallics* 2019, 38, 3931–3938; [PubMed: 34290468] c)Wang H; Li T; Zheng Z; Zhang L 'Efficient Synthesis of A-Allylbutenolides from Allyl Ynoates Via Tandem Ligand-Enabled Au(I) Catalysis and the Claisen Rearrangement' *ACS Catal.* 2019, 9, 10339–10342;d)Cheng X; Quintanilla CD; Zhang L 'Total Synthesis and Structure Revision of Diplobifuranyllone B' *J. Org. Chem* 2019, 84, 11054–11060; [PubMed: 31362500] e)Liao S; Porta A; Cheng X; Ma X; Zannoni G; Zhang L 'Bifunctional Ligand Enables Efficient Gold-Catalyzed Hydroalkenylation of Propargylic Alcohol' *Angew. Chem. Int. Ed* 2018, 57, 8250–8254;f)Li X; Wang Z; Ma X; Liu P.-n.; Zhang L 'Designed Bifunctional Phosphine Ligand-Enabled Gold-Catalyzed Isomerizations of Ynamides and Allenamides: Stereoselective and Regioselective Formation of 1-Amido-1,3-Dienes' *Org. Lett* 2017, 19, 5744–5747; [PubMed: 29035053] g)Li X; Liao S; Wang Z; Zhang L 'Ligand-Accelerated Gold-Catalyzed Addition of in Situ Generated Hydrazoic Acid to Alkynes under Neat Conditions' *Org. Lett* 2017, 19, 3687–3690. [PubMed: 28696717]
- (10)a). Oudeyer S; Brière J-F; Levacher V 'Progress in Catalytic Asymmetric Protonation' *Eur. J. Org. Chem* 2014, 2014, 6103–6119;b)Fu N; Zhang L; Luo S 'Catalytic Asymmetric Enamine Protonation Reaction' *Org. Biomol. Chem* 2018, 16, 510–520; [PubMed: 29302677] c)Kingston C; James J; Guiry PJ 'Development of and Recent Advances in Pd-Catalyzed Decarboxylative Asymmetric Protonation' *J. Org. Chem* 2019, 84, 473–485; [PubMed: 30376624] d)Phelan JP; Ellman JA 'Conjugate Addition–Enantioselective Protonation Reactions' *Beilstein Journal of Organic Chemistry* 2016, 12, 1203–1228. [PubMed: 27559372]
- (11)a). Grrirane A; Álvarez E; García H; Corma A 'Catalytic Activity of Cationic and Neutral Silver(I)–Xphos Complexes with Nitrogen Ligands or Tolylsulfonate for Mannich and Aza-Diels–Alder Coupling Reactions' *Chem. Eur. J* 2016, 22, 340–354; [PubMed: 26598792] b)Pérez-Galán P; Delpont N; Herrero-Gómez E; Maseras F; Echavarren AM 'Metal–Arene Interactions in Dialkylbiarylphosphane Complexes of Copper, Silver, and Gold' *Chem. Eur. J* 2010, 16, 5324–5332. [PubMed: 20394085]

- (12)a). Higashi T; Kusumoto S; Nozaki K 'Cleavage of Si–H, B–H, and C–H Bonds by Metal–Ligand Cooperation' *Chem. Rev* 2019, 119, 10393–10402; [PubMed: 31408323]  
b)Khusnutdinova JR; Milstein D 'Metal–Ligand Cooperation' *Angew. Chem. Int. Ed* 2015, 54, 12236–12273;c)Gunanathan C; Milstein D 'Metal–Ligand Cooperation by Aromatization–Dearomatization: A New Paradigm in Bond Activation and “Green” Catalysis' *Acc. Chem. Res* 2011, 44, 588–602. [PubMed: 21739968]
- (13)a). Guo J; Mao J 'Asymmetric Henry Reaction Catalyzed by Bifunctional Copper-Based Catalysts' *Chirality* 2009, 21, 619–627; [PubMed: 18798286] b)Lang K; Park J; Hong S 'Development of Bifunctional Aza-Bis(Oxazoline) Copper Catalysts for Enantioselective Henry Reaction' *J. Org. Chem* 2010, 75, 6424–6435; [PubMed: 20822170] c)Boobalan R; Lee G-H; Chen C 'Copper Complex of Aminoisoborneol Schiff Base Cu<sub>2</sub>(Sbaib-D)<sub>2</sub>: An Efficient Catalyst for Direct Catalytic Asymmetric Nitroaldol (Henry) Reaction' *Adv. Synth. Catal.* 2012, 354, 2511–2520;d)Zhao L; Ma Y; Duan W; He F; Chen J; Song C 'Asymmetric B-Boration of A,B-Unsaturated N-Acyloxazolidinones by [2.2]Paracyclophane-Based Bifunctional Catalyst' *Org. Lett* 2012, 14, 5780–5783; [PubMed: 23131139] e)Caron A; Morin É; Collins SK 'Bifunctional Copper-Based Photocatalyst for Reductive Pinacol-Type Couplings' *ACS Catal.* 2019, 9, 9458–9464;f)Das S; Sinha S; Samanta D; Mondal R; Chakraborty G; Brandaõ P; Paul ND 'Metal–Ligand Cooperative Approach to Achieve Dehydrogenative Functionalization of Alcohols to Quinolines and Quinazolin-4(3h)-Ones under Mild Aerobic Conditions' *J. Org. Chem* 2019, 84, 10160–10171. [PubMed: 31327228]
- (14). Satyanarayana T; Abraham S; Kagan HB 'Nonlinear Effects in Asymmetric Catalysis' *Angew. Chem., Int. Ed* 2009, 48, 456–494.
- (15). Kina A; Iwamura H; Hayashi T 'A Kinetic Study on Rh/Binap-Catalyzed 1,4-Addition of Phenylboronic Acid to Enones: Negative Nonlinear Effect Caused by Predominant Homochiral Dimer Contribution' *J. Am. Chem. Soc* 2006, 128, 3904–3905. [PubMed: 16551086]
- (16). Xue X-S; Li X; Yu A; Yang C; Song C; Cheng J-P 'Mechanism and Selectivity of Bioinspired Cinchona Alkaloid Derivatives Catalyzed Asymmetric Olefin Isomerization: A Computational Study' *J. Am. Chem. Soc* 2013, 135, 7462–7473. [PubMed: 23638651]



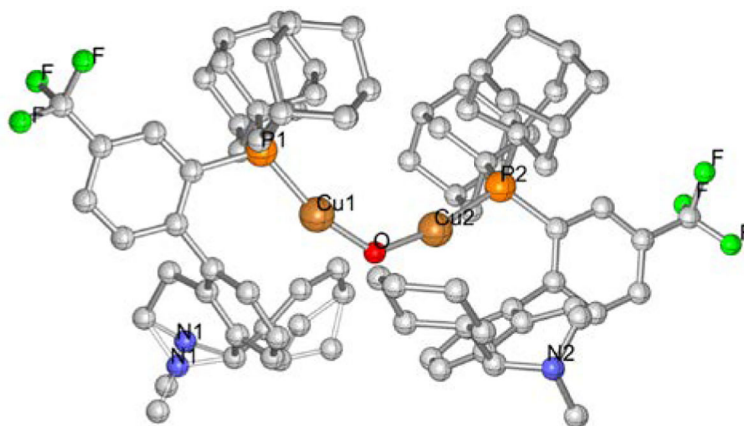
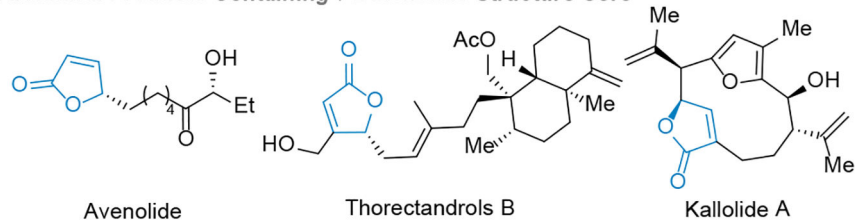
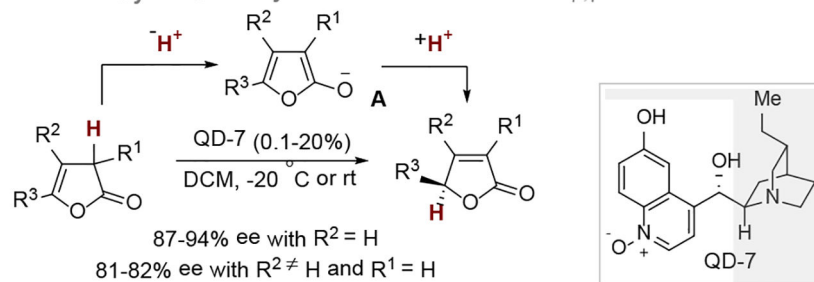


**Figure 1.** CYL drawing of the dimeric Cu(I) complex. The crystal solvent molecules, i.e., one MeCN and three Et<sub>2</sub>O, are omitted for clarity.  $\angle\text{P1-Cu1-O} = 163.2^\circ$  and  $\angle\text{P2-Cu2-O} = 167.8^\circ$

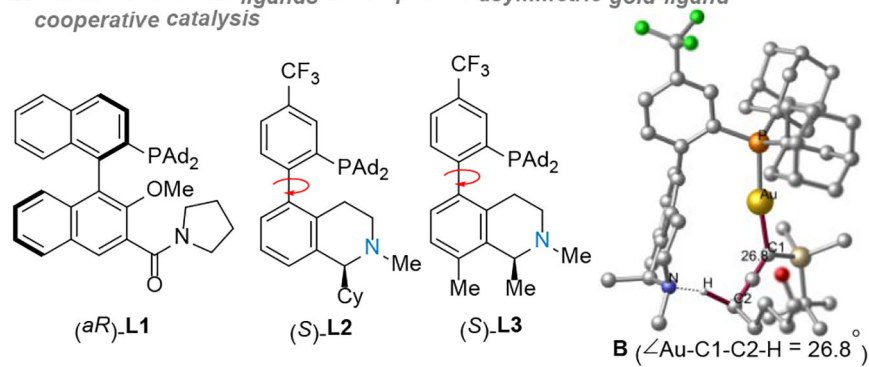
**A. Natural Products Containing  $\gamma$ -Butenolide Structure Core**



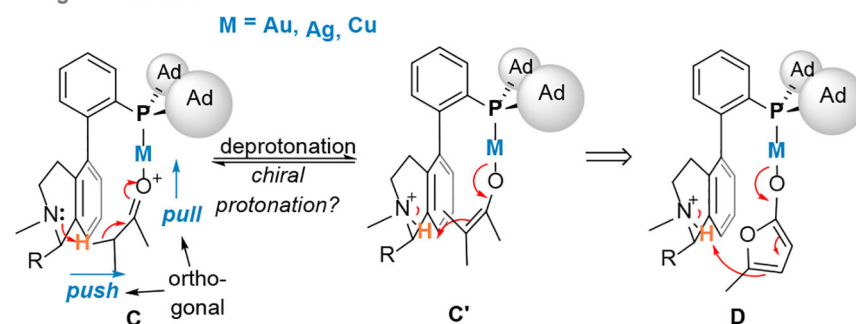
**B. Prior work by Deng on asymmetric isomerization of  $\beta,\gamma$ -butenolides**



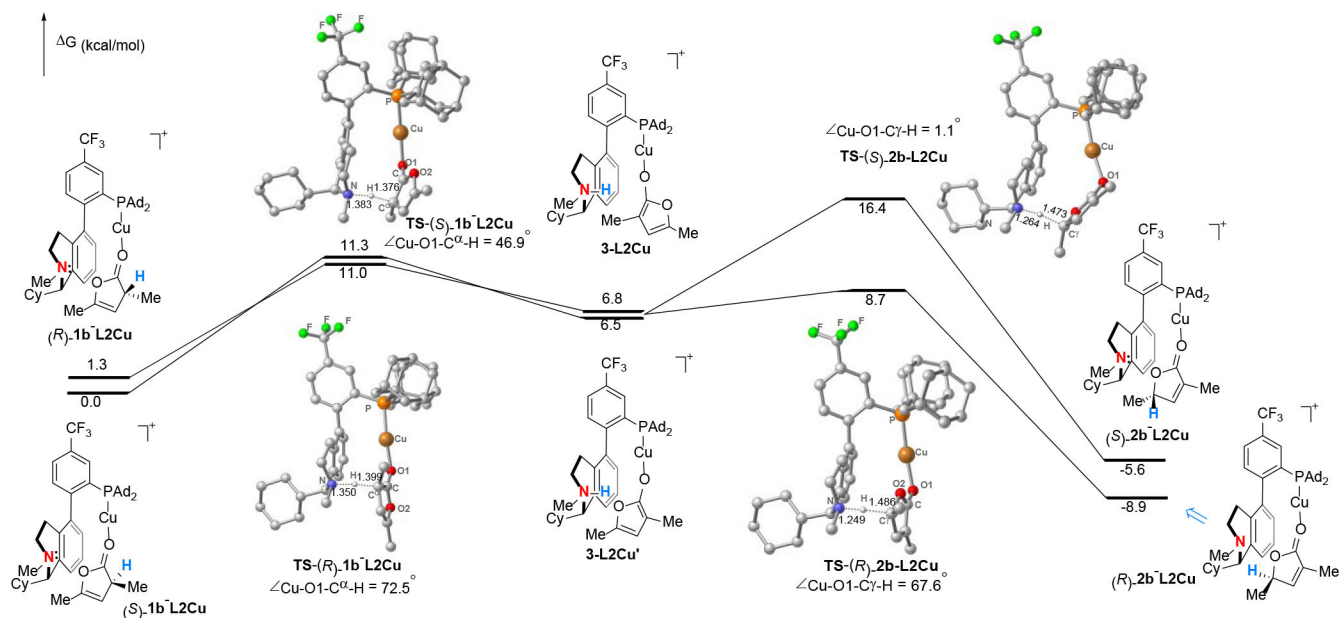
**C. Chiral bifunctional ligands developed for asymmetric gold-ligand cooperative catalysis**



**D. Ligand-enabled soft enolization**



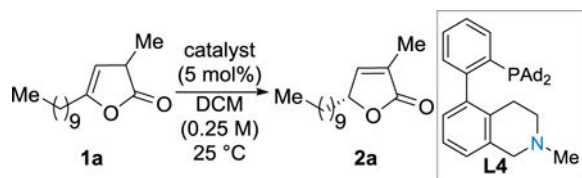
**Scheme 1.**  
Butenolide natural product and reaction design

**Scheme 2.**

DFT Calculated energetics of the reaction forming **2b** at the PBE1PBE/6-31(d,p)/6-311g(d,p)(P)/SDD(Cu) level of theory with SMD (DCM).

Table 1.

## Reaction Condition Optimization



Entry <sup>a</sup>	Catalyst	Time (h)	Conv.	Yield (%) <sup>b</sup>	ee (%) <sup>c</sup>
1	[Cu(MeCN) <sub>4</sub> ] <sup>+</sup> PF <sub>6</sub> <sup>-</sup>	3	2	NA	NA
2	[Cu(MeCN) <sub>4</sub> ] <sup>+</sup> PF <sub>6</sub> <sup>-</sup> /Et <sub>3</sub> N	3	3	NA	NA
3	[JohnPhosCu(MeCN)] <sup>+</sup> PF <sub>6</sub> <sup>-</sup> /Et <sub>3</sub> N	16	35	6	NA
4	[Cu(MeCN) <sub>4</sub> ] <sup>+</sup> PF <sub>6</sub> <sup>-</sup> / <b>L4</b>	3	100	99	NA
5	[Cu(MeCN) <sub>4</sub> ] <sup>+</sup> PF <sub>6</sub> <sup>-</sup> /( <i>S</i> )- <b>L2</b>	3	100	99	98
6	[Cu(MeCN) <sub>4</sub> ] <sup>+</sup> PF <sub>6</sub> <sup>-</sup> /( <i>S</i> )- <b>L3</b>	3	100	99	94
7	[( <i>S</i> )- <b>L2</b> Cu(MeCN)] <sup>+</sup> PF <sub>6</sub> <sup>-</sup>	1	100	99	97
<b>8</b> <sup>d</sup>	[( <i>S</i> )- <b>L2</b> Cu(MeCN)] <sup>+</sup> PF <sub>6</sub> <sup>-</sup>	<b>0.5</b>	<b>100</b>	<b>99</b> <sup>e</sup>	<b>98</b>
9 <sup>d,f</sup>	{[( <i>S</i> )- <b>L2</b> Cu] <sub>2</sub> (H <sub>2</sub> O)} <sub>2</sub> <sup>+</sup> (PF <sub>6</sub> <sup>-</sup> ) <sub>2</sub>	0.5	100	99	98
10	( <i>S</i> )- <b>L2</b>	3	NA	NA	NA
11	Cu(OTf) <sub>2</sub> or Cu(hfac) <sub>2</sub> /( <i>S</i> )- <b>L2</b>	24	<5	<5	NA
12	( <i>S</i> )- <b>L2</b> AuCl / NaBARF <sub>4</sub> (10 mol%)	0.5	100	99	99
13	[Ag(MeCN) <sub>2</sub> ] <sup>+</sup> BARF <sub>4</sub> <sup>-</sup> /( <i>S</i> )- <b>L2</b>	0.5	100	99	98
14 <sup>g</sup>	[( <i>S</i> )- <b>L2</b> Cu(MeCN)] <sup>+</sup> PF <sub>6</sub> <sup>-</sup>	1	100	92 <sup>h</sup>	99

<sup>a</sup>Reaction was performed at 0.05 mmol scale in 1-dram vials.

<sup>b</sup>The NMR yield is calculated by assuming that the triplet at around 0.87 ppm corresponds to the terminal methyl groups of all compounds.

<sup>c</sup>Detected using chiral HPLC.

<sup>d</sup>Under Ar atmosphere.

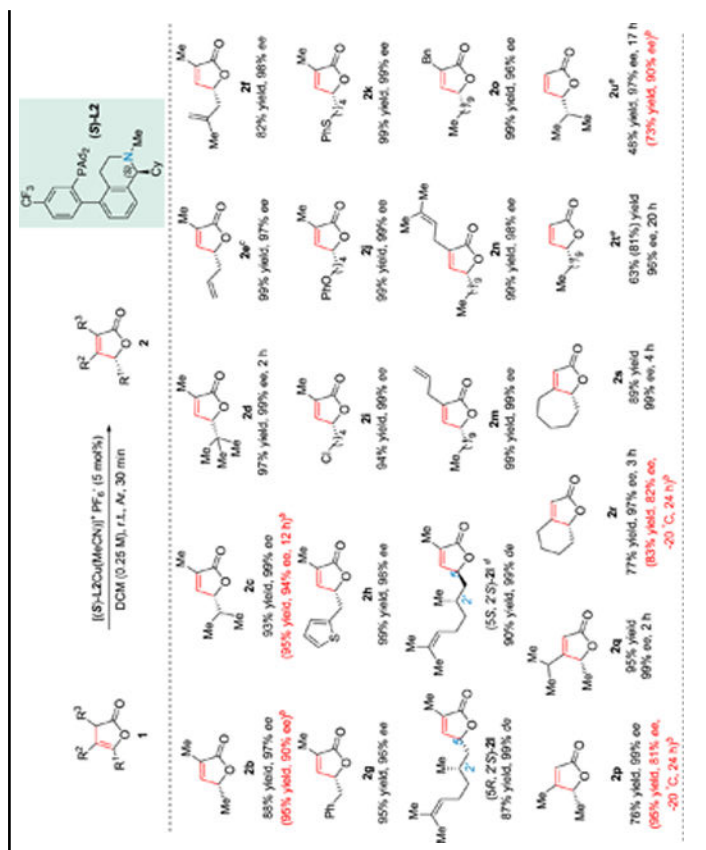
<sup>e</sup>Isolated yield.

<sup>f</sup>Reaction was performed with 2.5 mol% catalyst.

<sup>g</sup>Reaction was performed with 1 mol % of catalyst.

<sup>h</sup>0.99 g product isolated.

Table 2.

Reaction Scope <sup>a</sup>

<sup>a</sup>Reaction was performed in 2-dram sealed vials under argon at room temperature. Yield calculated based on the conversion was included in parentheses. Reaction scale is 0.3 mmol and reaction time is 0.5 h if not specified.

<sup>b</sup>The result reported in ref. 5.

<sup>c</sup>Reaction was performed at 0.15 mmol scale.

<sup>d</sup>5 mol% (*R*)-**L2Cu**(MeCN)PF<sub>6</sub> was used.

<sup>e</sup>Reaction was performed at 40 °C.